The effect of aerosol vertical profiles on satellite-estimated surface particle sulfate concentrations

Yang Liu [a,*], Zifeng Wang [b], Jun Wang [c], Richard A. Ferrare [d], Robert K. Newsom [e], Ellsworth J. Welton [f]

[a] Emory University, Rollins School of Public Health, Department of Environmental Health, 1518 Clifton Road NE, Atlanta, GA 30322, United States
[b] Chinese Academy of Sciences, Institute of Remote Sensing Applications, Beijing, China
[c] University of Nebraska, Department of Earth and Atmospheric Sciences, Lincoln, NE
[d] NASA Langley Research Center, Hampton, VA, United States
[e] Pacific Northwest National Laboratory, Richland, WA, United States
[f] NASA Goddard Space Flight Center, Greenbelt, MD, United States

ARTICLE INFO

ABSTRACT

The aerosol vertical distribution is an important factor in determining the relationship between satellite retrieved aerosol optical depth (AOD) and ground-level fine particle pollution concentrations. We evaluate how aerosol profiles measured by ground-based lidar and simulated by models can help improve the association between AOD retrieved by the Multi-angle Imaging Spectroradiometer (MISR) and fine particle sulfate (SO4) concentrations using matched data at two lidar sites. At the Goddard Space Flight Center (GSFC) site, both lidar and model aerosol profiles marginally improve the association between SO4 concentrations and MISR fractional AODs, as the correlation coefficient between cross-validation (CV) and observed SO4 concentrations changes from 0.87 for the no-scaling model to 0.88 for models scaled with aerosol vertical profiles. At the GSFC site, a large amount of urban aerosols resides in the well-mixed boundary layer so the column fractional AODs are already excellent indicators of ground-level particle pollution. In contrast, at the Atmospheric Radiation Measurement Program (ARM) site with relatively low aerosol loadings, scaling substantially improves model performance. The correlation coefficient between CV and observed SO4 concentrations is increased from 0.58 for the no-scaling model to 0.76 in the GEOS-Chem scaling model, and the model bias is reduced from 17% to 9%. In summary, despite the inaccuracy due to the coarse horizontal resolution and the challenges of simulating turbulent mixing in the boundary layer, GEOS-Chem simulated aerosol profiles can still improve methods for estimating surface aerosol (SO4) mass from satellite-based AODs, particularly in rural areas where aerosols in the free troposphere and any long-range transport of aerosols can significantly contribute to the column AOD.

© 2010 Elsevier Inc. All rights reserved.

1. Introduction

In addition to providing extensive impacts on our climate and environment (Kaufman et al., 2002), ambient aerosols can bring adverse effects on public health. Epidemiologic studies around the world have found strong links between chronic exposure to $PM_{2.5}$ (particulate matter with aerodynamic diameter less than 2.5 μm) and increased respiratory and cardiovascular morbidity and mortality (Pope & Dockery, 2006). As one of the major constituents of $PM_{2.5}$, sulfate (SO4) has been also linked to adverse health impacts (Willis et al., 2003). Studying the impacts of SO4 as well as other $PM_{2.5}$ constituents on human health is important in determining air quality standards and control policies for $PM_{2.5}$. Current ground monitoring networks in the United States such as the Chemical Speciation Network (CSN) operated by the U.S. Environmental Protection Agency (EPA) and the Interagency Monitoring of Protected Visual Environments (IMPROVE) network do not have sufficient spatial coverage to study the long-range transport and regional spatial patterns of SO4.

The Multi-angle Imaging Spectroradiometer (MISR) aboard the Terra satellite can distinguish particles based on size, shape and single scattering albedo (Kahn et al., 2001). MISR-retrieved aerosol optical depth (AOD) and aerosol microphysical properties have been used to develop statistical models to estimate ground-level $PM_{2.5}$ concentrations (Liu et al., 2007a,b). Previous research showed that the aerosol vertical distribution is an important source of uncertainty impacting the relationship between AOD and $PM_{2.5}$ (Liu et al., 2009). Aerosol vertical profiles can be simulated by atmospheric chemical transport models or measured by spaceborne, airborne, or ground lidars (Schmid et al., 2006). Model-simulated aerosol profiles such as those from the GEOS-Chem model (Park et al., 2004) have complete temporal and spatial coverage, and have been shown to substantially strengthen the association between MISR AOD and SO4 concentrations

* Corresponding author. Tel.: +1 404 727 2131; fax: +1 404 727 8744.
E-mail address: yang.liu@emory.edu (Y. Liu).

(Liu et al., 2009). However, the horizontal resolution of GEOS-Chem is 100–200 km, much coarser than that of the MISR product (17.6 km). A few studies have explored the value of ground-based lidar data in improving the correlation between satellite AOD and PM$_{2.5}$ (Engel-Cox et al., 2006). Although a well-calibrated ground-based lidar can provide accurate aerosol profiles with high temporal and vertical resolutions, it does not have the spatial coverage necessary to support regional scale studies.

In this analysis, we compare the capabilities of ground-based lidar and model-simulated aerosol vertical profiles in improving the AOD–SO4 association. We first compare GEOS-Chem simulated aerosol profiles with matched lidar aerosol profiles at two lidar sites. Then both profiles are used in a statistical model together with MISR AOD to estimate ground-level SO4 concentrations. A description of data and methods is given in Section 2, the results of profile comparison, statistical analysis and discussion are given in Section 3, and conclusions are presented in Section 4.

2. Data and method

2.1. Data processing

MISR data, GEOS-Chem aerosol profiles, and ground-based SO4 measurements must be matched to lidar sites to ensure accurate comparisons and to develop the statistical models. The Micro-Pulse Lidar Network (MPLNET) of the National Aeronautics and Space Administration (NASA) is a federated network of lidar systems designed to continuously measure long-term aerosols and clouds vertical structures (Campbell et al., 2002). Constrained by coincident AOD measurements, an MPL can estimate aerosol extinction profiles every 20 min at 523 nm wavelength with a vertical resolution of 75 m during daytime in cloud-free conditions (Welton et al., 2002). The Level 1.5a aerosol extinction profiles measured at the Goddard Space Flight Center (GSFC) site (39.016 N, 76.867 W) from 2001 to 2007 were collected for this study. The GSFC site is located in the densely populated Washington D.C. area with high PM$_{2.5}$ pollution levels (Fig. 1). The Raman lidar at the Atmospheric Radiation Measurement Program (ARM) Southern Great Plains (SGP) site (36.609 N, 97.487 W), is a fully automated lidar system designed for continuous profiling of atmospheric water vapor, clouds and aerosols. The ARM Raman lidar is surrounded by the cattle pasture and wheat fields southeast of Lamont, Oklahoma with flat terrain, large seasonal weather variations and no major local emission sources. Measurements from this lidar are used to determine the aerosol vertical distribution for a rural background location (Fig. 1). The ARM lidar operates at a wavelength of 355 nm and measures backscatter profiles in 10 separate detection channels. Prior to a major system upgrade in 2004 (Ferrare et al., 2006), aerosol extinction profiles at 355 nm were recorded at 10 min frequency and 39 m vertical resolution. After

2004, the resolutions were improved to 10 min and 15 m (Newsom et al., 2009). The Raman lidar data from 2001 to 2008 were collected from the ARM data archive (http://www.archive.arm.gov/). We excluded data from mid 2002 to the end of 2003 due to the high random noise caused by lidar sensitivity degradation (Ferrare et al., 2006). In addition, positive values greater than 0.4 km^{-1} in the extinction profiles were removed to prevent outliers from entering the modeling process (Schmid et al., 2009). Daily gravimetrically based SO4 concentrations (parameter code 88403) measured at locations close to the two lidar sites from 2001 to 2008 were collected from the U.S. EPA Air Quality System (http://www.epa.gov/ttn/airs/airsaqs). Three sites within 30 km of the GSFC site and three sites within 150 km of the ARM site were selected to match to the lidar sites.

The Level 2 MISR aerosol data product (version 22) from 2001 to 2008 was obtained from the NASA Langley Research Center Atmospheric Science Data Center (http://eosweb.larc.nasa.gov/), and matched to the selected EPA sites. MISR aerosol data have a spatial resolution of 17.6 km and sampling frequency of approximately nine days at mid latitudes (Diner et al., 2002). These data are most sensitive to particles in a diameter range of 0.05 to 2 μm (Kahn et al., 1998), corresponding to the size range of PM$_{2.5}$. Eight approximately orthogonal aerosol components are predefined to construct 74 aerosol mixtures. MISR fractional AOD values of these components, each of which is defined as the average contribution of a component to total AOD in all successful aerosol mixtures identified by the MISR aerosol retrieval algorithm, contain more information of the ambient aerosol speciation than the total AOD, and they can be used as individual predictors of PM$_{2.5}$ and its major constituents (Liu et al., 2007a).

The GEOS-Chem model is a global 3-D chemistry and transport model (CTM) driven by assimilated meteorological observations from the Goddard Earth Observing System (GEOS) at the NASA Global Modeling and Assimilation Office (GMAO) (Bey et al., 2001). GEOS-Chem can simulate the mass loadings of all major aerosol species at 3-h intervals and 2° × 2.5° horizontal resolution or higher. Depending on the version of the meteorological data (e.g., GEOS-4 or GEOS-5 in the current analysis), the simulations can be conducted at 20 or 37 vertical layers in the troposphere. GEOS-Chem AOD profiles are calculated from the simulated aerosol dry mass concentrations, and particle growth with increased relative humidity is also taken into account. The simulated AOD profiles (averaged between 10 am and 4 pm local time) from 2001 to 2008 were used in this study, of which 2001 to 2006 data (model version 7-04-12) are driven by GEOS-4 meteorological fields, and 2007 and 2008 data (model version 8-01-01) are driven by GEOS-5 meteorological fields.

Because the majority of aerosol mass resides in the lower troposphere, the lidar backscattered signals from the upper troposphere (more than 7–8 km above the surface) often contain little aerosol information and may have more uncertainties due to the solar background. According to Welton et al. (2002) and Campbell et al. (2002), we set an altitude of 8 km as the upper altitude limit for both lidars, and used only the extinction profiles below this altitude to scale the MISR column AOD. For consistency, this altitude limit is also applied to GEOS-Chem AOD profiles, which corresponds to the lower 10 layers for GEOS-4 and 27 layers for GEOS-5. The aerosol contribution above 8 km to column AOD is on average ~3% at the GSFC site and ~5% at the ARM site based on GEOS-Chem simulation results. Therefore, discarding the aerosol loading above 8 km will have a minimal impact on the analysis. Since our goal is to evaluate whether the horizontal and vertical resolutions of aerosol profiles have a significant impact on the AOD-SO4 association, we average the lidar aerosol profiles to match GEOS-Chem vertical layers.

2.2. Model development

In previous studies (Liu et al., 2004, 2009; van Donkelaar et al., 2006), GEOS-Chem simulated profiles have successfully improved the
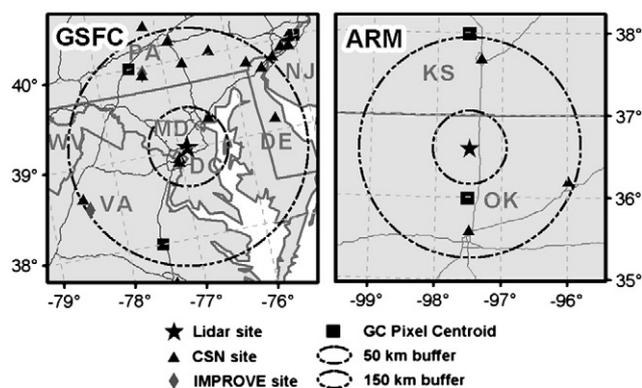

Fig. 1. Surrounding environment of the two ground-based lidar sites.

AOD–PM$_{2.5}$ correlation at continental to global scales. To take advantage of MISR's ability to distinguish particle species, fractional AODs are calculated using MISR aerosol component and mixture information as described in Liu et al. (2007a). Both GEOS-Chem and lidar aerosol profiles are used to calculate the planetary boundary layer (PBL) portion of the fractional AODs (Eq. (1)). We define the PBL AOD proportion as the ratio of AOD below GEOS-Chem daytime boundary layer height (on average 1.1 km above the ground at both lidar sites) to total AOD (i.e., from surface to 8 km altitude) for both GEOS-Chem and lidar aerosol profiles. We use these proportions to scale MISR column fractional AODs before developing the statistical models to estimate SO4 concentrations.

$$\text{MISR PBL AOD} = \text{MISR column AOD} \times \frac{\text{lidar(model) PBL AOD}}{\text{lidar(model) column AOD}} \quad (1)$$

The approximately orthogonal design of the eight MISR aerosol components enables us to include their fractional AODs as individual predictors in statistical models, which perform better than using total AOD as the sole predictor in estimating PM$_{2.5}$ speciation concentrations (Liu et al., 2007a,b). A generalized additive model (GAM) is developed for each scaling method (i.e., using lidar aerosol profiles to calculate MISR PBL fractional AODs based on Eq. (1) versus using GEOS-Chem aerosol profiles) at each site, with a general model structure shown in Eq. (2). A GAM expands the capability of traditional linear regression by allowing some or all predictor variables to have non-linear relationships with the dependent variable by using semi-parametric spline smoothers (Wood, 2004). A previous comparison between a GAM and a linear regression model over the whole continental U.S. shows the higher accuracy and stability of GAM in estimating SO4 concentrations (Liu et al., 2009). The left hand side of Eq. (2) (i.e., the dependent variable) is daily SO4 concentrations. On the right hand side, α is the overall model intercept, and f_i's are smooth terms for MISR fractional AODs in the PBL. As the reference, a similar GAM is also developed with column MISR fractional AODs as predictor variables. Final models are selected to include variables with a p-value less than 0.20. We validated our model using the k-fold cross-validation (CV) technique. In particular, after deciding which of the predictors to include in the final model using the whole dataset, we sequentially retained approximately 10% of the data (randomly selected) as the testing dataset, fitted the model to the remaining data, and then made predictions of daily SO4 concentrations at the testing dataset. Given the small sample sizes, we repeated the k-fold CV process 100 times and calculated the mean CV estimated SO4 concentrations to be compared with the observed SO4 concentrations. We estimated the model prediction precision by taking the square root of the mean squared CV prediction errors.

$$[SO4] = \alpha + \sum_{i=1}^{8} f_i(\text{MISR PBL fractional AOD}_i) \quad (2)$$

3. Result and discussion

3.1. Comparison of aerosol profiles

Fig. 2 shows similar patterns of monthly mean AOD values expressed as the percentage of annual mean AOD values at the lidar sites. Both sites have the highest monthly AOD in July and August (170–180% of annual mean at the GSFC site, and 150% at the ARM site). The lowest monthly AOD occurs in January and February (42% and 50% of annual mean respectively) at the GSFC site and in December and January (both 57% of annual mean) at the ARM SGP site. The slightly greater monthly AOD fluctuation at the GSFC site is probably caused by the stronger emissions locally and in surrounding densely populated areas.
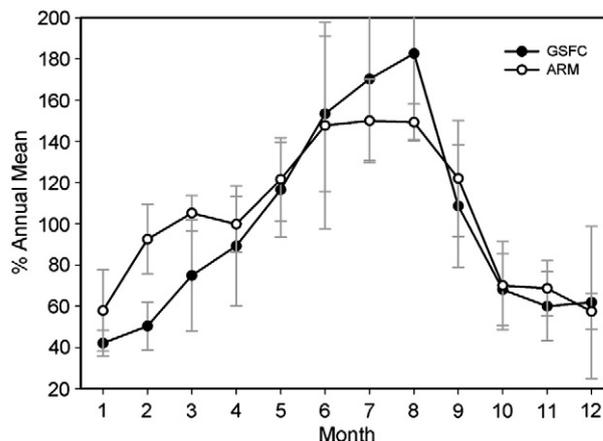

Fig. 2. Monthly column AOD trend at the GSFC and ARM sites expressed as percentage of annual mean AOD value. Vertical bars indicate standard deviation of the monthly deviation calculated from monthly AODs between 2001 and 2007.

Lidar aerosol profiles have much higher vertical resolutions than the GEOS-Chem model simulations, and GEOS-Chem and lidar extinction coefficients have systematic deviations due to their different wavelengths (ARM SGP Raman lidar at 355 nm, GSFC lidar at 532 nm, and GEOS-Chem simulations at 550 nm). To facilitate the comparison, we integrated the lidar extinction coefficients to calculate lidar AOD values in each GEOS-Chem model layer. Model fitting results for the GAMs with MISR PBL fractional AODs scaled by GEOS-Chem PM$_{2.5}$ extinction profiles (instead of by SO4 extinction profiles) are shown since preliminary analysis shows that they perform better. Fig. 3 shows the annual mean normalized GEOS-Chem and lidar aerosol profiles at both sites plotted on GEOS-4 vertical layers (results on GEOS-5 vertical layers are very similar, therefore not shown here). Normalization with column AOD (i.e., below 8 km altitude) was done so that the AOD values of all layers sum to unity. This process helps emphasize the comparison of the shape of aerosol vertical distributions and reduces the difference in AOD values due to wavelength differences. At the GSFC site, simulated aerosol profiles agree well with lidar measurements in the free troposphere above ~4 km. Notable differences appear in the lower atmospheric layers, where the lidar profile has its largest AOD contributions between 1 and 2 km altitude while model simulation has its largest AOD contributions between surface and 1 km altitude. At the ARM SGP site, the Raman lidar consistently observes larger AOD contributions between approximately 1.5 km and 6 km altitude. Simulated aerosol extinction coefficients decrease with altitude more rapidly than the lidar measurements, resulting in larger AOD contributions in layers below 1 km. Both the observed and simulated AOD profiles peak near 1 km altitude. Analysis of the extinction coefficients shows that lidar observes a well-mixed boundary layer below 2 km altitude with relatively uniform extinction coefficients. This phenomenon has been reported in previous lidar studies (Schmid et al., 2009). The version of GEOS-Chem used for this study assumes that all surface emissions are fully mixed within the PBL at each simulation time step (Lin & McElroy, 2010), which can be substantially shallower than 1 km during the early hours of the day. This might cause the simulated aerosol extinction coefficients to peak at the bottom layer and decrease rapidly with altitude, resulting in a larger AOD contribution near the surface. The day-to-day fluctuation of AOD contributions at this altitude range measured by the standard deviation of daily normalized AOD values (shown as horizontal error bars at the center of each layer in Fig. 3) is much wider at the ARM SGP site than at the GSFC site, which likely shows the relatively large influence of high-altitude transport events on total aerosol loading in clean rural areas.

The average PBL AOD proportions according to Eq. (1) are similar for the lidar and model at both sites. At the GSFC site, it is 0.61 ± 0.23
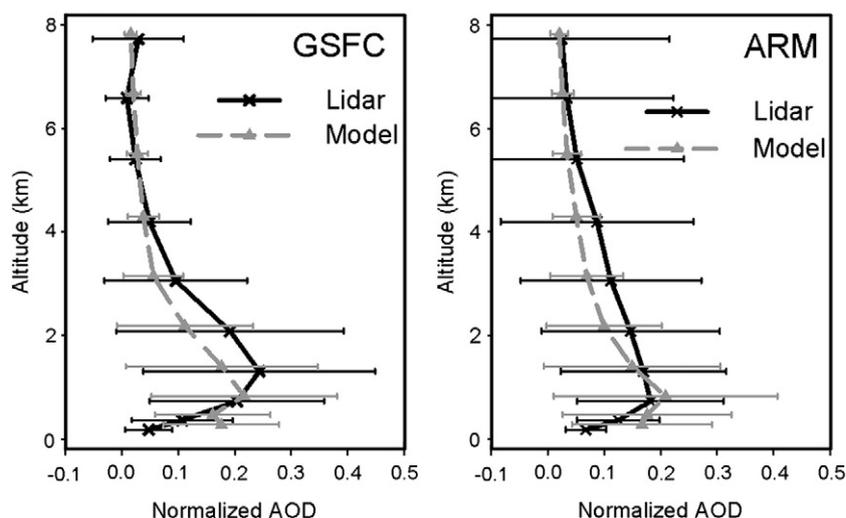
Fig. 3. Comparisons between the mean normalized aerosol profiles of lidars (355 nm for ARM lidar, and 535 nm for GSFC lidar) and GEOS-Chem (550 nm) at the GSFC site (left) and the ARM site (right). Lidar profiles are shown as black solid lines, GEOS-Chem profiles are shown as gray dashed lines. Horizontal error bars at each latitude are one standard deviation of daily normalized AOD values.

measured by lidar, and 0.62 ± 0.15 estimated by GEOS-Chem ($N = 1007$ for all lidar profiles matched with GEOS-Chem simulation results). At the ARM site, it is 0.50 ± 0.26 by lidar and 0.55 ± 0.17 by GEOS-Chem ($N = 1171$). Seasonally, both sites have the highest PBL AOD proportion in the fall and winter (0.68 ± 0.13 at GSFC, and 0.62 ± 0.14 at ARM), and lowest in the spring (0.52 ± 0.12 at GSFC and 0.46 ± 0.13 at ARM). To assess the day-to-day difference between the two lidar aerosol profiles, we calculated the relative differences between the lidar observed and GEOS-Chem simulated PBL AOD fractions as:

$$\text{Relative Difference} = 2 \times \left| \frac{\text{lidar AOD fraction} - \text{GC AOD fraction}}{\text{lidar AOD fraction} + \text{GC AOD fraction}} \right|. \quad (3)$$

The median relative difference is 24% at the GSFC site, and 36.5% at the ARM site. These discrepancies could be partially attributed to the much coarser GEOS-Chem modeling grid which has limited capabilities to resolve the temporal fluctuation of aerosol loadings at a finer (sub-grid) spatial scale observed by lidar as well as the full boundary layer mixing assumption of the model (Lin & McElroy, 2010).

3.2. Effects of aerosol vertical profiles on GAM performance

There are 76 data records at the GSFC site after matching MISR aerosol data with EPA observations and lidar data (GEOS-Chem simulated aerosol profiles have complete temporal coverage), with more records in the fall (28) and fewer records in the winter (10). Table 1 provides a summary of model fitting statistics. The correlation coefficient between the mean CV predicted (i.e., averaged over 100 repetitions) and the observed SO4 concentrations ranges from 0.87 (no scaling) to 0.88 (both lidar scaling and GEOS-Chem scaling). The average root mean square prediction error (RMSPE) ranges from 2.8 μg/m³ (no scaling) to 3.2 μg/m³ (lidar scaling). Fig. 4 shows that mean CV predicted SO4 concentrations using the GEOS-Chem scaling method have a smaller overall bias as measured by the linear regression slope (5%) as compared to the no-scaling method (8%) and lidar scaling method (6%). All three models can predict annual mean SO4 concentrations accurately. The mean CV predicted SO4 concentrations are 5.1 μg/m³, 5.3 μg/m³, and 5.0 μg/m³, for the no scaling, lidar scaling, and GEOS-Chem scaling methods, respectively. As a comparison, the mean observed SO4 concentration is 5.0 μg/m³. Comparing with the no-scaling approach, both lidar and model aerosol profiles provide marginal improvements, with the model aerosol

profiles performing slightly better. This finding holds true even when the two highest SO4 concentrations are excluded.

There are 54 data records at the ARM SGP site after the matching process, with more data records in the fall (19) and fewer records in the winter (6). The correlation coefficients between the mean CV predicted and the observed SO4 concentrations are 0.60 (no scaling), 0.65 (lidar scaling), and 0.59 (GEOS-Chem scaling). The average RMSPEs of all three models are very similar (1.6–1.7 μg/m³, Table 1). When compared with the CV results, the three GAMs have an average of approximately 17% low bias. All three models can predict annual mean SO4 concentrations accurately. The mean CV predicted SO4 concentrations are 2.9 μg/m³, 2.8 μg/m³, and 2.8 μg/m³, for the no scaling, lidar scaling, and GEOS-Chem scaling methods, respectively. As a comparison, the mean observed SO4 concentration is 2.9 μg/m³. The lidar and model aerosol profiles do not seem to improve the correlation between CV predicted and observed SO4 concentrations. It should be noted that the smaller sample size at the ARM site is not sufficient to support a full GAM with sufficient smoothness settings for the predictor variables, hence restrains model predicting power. Relaxing the matching criteria to include all matched MISR/EPA/GEOS-Chem data in all years results in a larger dataset ($N = 136$) with a more balanced temporal coverage (41 data records in the fall, and 29 in the winter). As shown in Fig. 5 (center and right plots), scaling substantially improves model performance. The correlation coefficient between the CV predicted and the observed SO4 concentrations

Table 1
Linear correlation coefficients between GAM fitted and observed SO4 concentrations at the two lidar sites.

Site	GSFC		ARM			
	$N = 76$		$N = 54$[a]		$N = 136$[b]	
Parameter	r[c]	RMSPE[d] (μg/m³)	r	RMSPE (μg/m³)	r	RMSPE (μg/m³)
Model 1: no scaling	0.87	2.8	0.60	1.6	0.58	1.6
Model 2: lidar scaling	0.88	3.2	0.65	1.6	N/A	N/A
Model 3: GC scaling	0.88	3.0	0.59	1.7	0.76	1.4

[a] MISR/lidar/GEOS-Chem matched dataset with July 2002–December 2003 data removed.
[b] MISR/GEOS-Chem matched dataset for all years.
[c] Correlation coefficient between mean cross-validation predicted daily SO4 concentrations (i.e., averaged over 100 repetitions) and EPA observations.
[d] Average square root of mean squared prediction error over 100 repetitions of cross-validation.
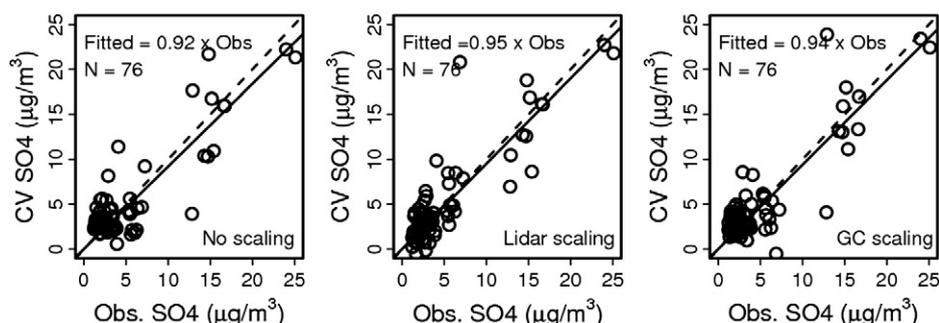
Fig. 4. Scatterplots of mean CV SO4 concentrations (i.e., averaged over 100 repetitions) versus U.S. EPA observations with different AOD scaling methods at the GSFC site. The solid line represents simple linear regression results with intercept excluded. The 1:1 line is displayed as a dashed line for reference. *N* is sample size. Left: column fractional MISR AODs as predictors; center: lidar-scaled PBL fractional MISR AODs as predictors; right: GC-scaled fractional MISR AODs as predictors.

increases from 0.58 in the no-scaling model to 0.76 in the GEOS-Chem scaling model. Model bias is reduced from 17% to 9%. The average root mean square prediction error (RMSPE) drops from 1.6 μg/m³ to 1.4 μg/m³ (Table 1).

The factors that can affect the AOD–PM association have been discussed in detail elsewhere (Liu et al., 2005). Our discussion here focuses on the different effects of aerosol vertical profiles observed at the two lidar sites. The densely populated DC–Maryland region is known to have a high level of SO4 pollution due to local emissions and substantial long-range transport from the Ohio River Valley (ORV) through southern Pennsylvania. Back trajectory analysis shows that most trajectory ensembles descend from around 2 km at the ORV over the course of three days, and encounter the daytime boundary layer in the Baltimore region (Fairlie et al., 2009). SO4 concentration in the free troposphere is low most of the time at the GSFC site without a significant temporal fluctuation as confirmed by the low normalized AOD values and the small standard deviation above 4 km altitude in Fig. 3. The average SO4 concentration in the fully matched GSFC dataset is 4.9 μg/m³, much higher than the ARM site (2.9 μg/m³). Albeit the large temporal variation of aerosol loadings, the dominance of sulfate particles trapped in a well-mixed boundary layer provides the ideal condition for AOD to be an effective predictor of ground-level SO4 concentrations. In fact, our analysis shows that the total column MISR AOD is highly correlated with SO4 concentrations ($r = 0.81$). Therefore, observed or modeled aerosol vertical profiles can only provide limited improvement to the AOD–SO4 association at this location. In contrast, the ARM SGP site is a rural site without any major emission sources nearby, and the average SO4 concentration is substantially lower than the GSFC site. The much larger standard deviation in the free troposphere portion of the mean aerosol profile at the ARM SGP site shown in Fig. 3 suggests the impact of the long-range transport event (such as sporadic transport of smoke particles from Yucatan Peninsula in each Spring (Wang et al., 2006)) that may influence the particle loading at the ground level. Therefore, calculating the PBL portion of fractional AODs using aerosol vertical profiles is an effective method of strengthening the AOD–SO4 association.

4. Conclusion

We match ground-based lidar aerosol vertical profiles with GEOS-Chem simulated aerosol profiles, MISR retrieved aerosol microphysical properties, and EPA SO4 concentration measurements at the GSFC and ARM lidar sites. Statistical models are developed to evaluate the improvement brought by aerosol profiles to MISR's capabilities of predicting ground-level SO4 concentrations. In general, there is a reasonable agreement between average normalized GEOS-Chem and lidar AOD profiles while their differences are larger at the daily level. At both sites, MISR fractional AODs are highly significant predictors of surface SO4 concentrations with less prediction bias at the GSFC site than at the ARM site. At the GSFC site, aerosol profiles only marginally improve the AOD–SO4 association as column AOD is already an excellent indicator of ground-level particle pollution. Despite the inaccuracy caused by the coarse horizontal resolution and imperfect emissions assumptions in the GEOS-Chem model, GEOS-Chem aerosol profiles can still substantially enhance the predicting power of our statistical models and reduce the overall model bias at the ARM site. Data matching results in a dataset too small to fit a full GAM using lidar data. As a result, we are unable to directly evaluate the effectiveness of the more accurate lidar aerosol profiles in improving MISR's capability to estimate SO4 concentrations. To obtain a larger dataset with more diverse aerosol profiles, future research may take advantage of aerosol profiles retrieved by the Cloud-Aerosol Lidar and Infrared Pathfinder Satellite Observation (CALIPSO) and align them with the Moderate Resolution Imaging Spectroradiometer (MODIS) AOD data.
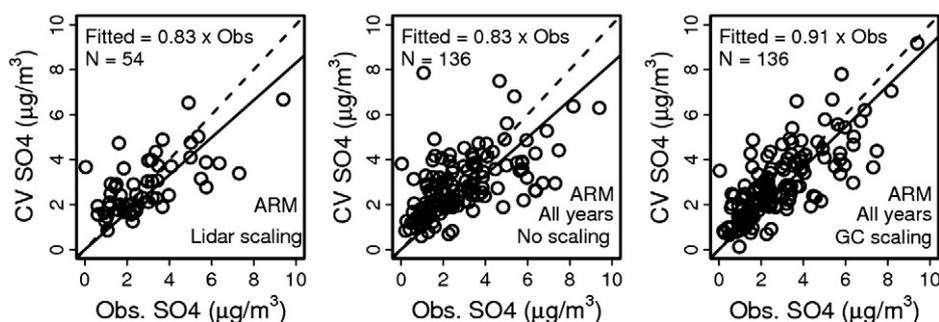
Fig. 5. Scatterplots of mean CV SO4 concentrations (i.e., averaged over 100 repetitions) versus U.S. EPA observations with different AOD scaling methods at the ARM site. The solid line represents simple linear regression results with intercept excluded. The 1:1 line is displayed as a dashed line for reference. *N* is sample size. Left: lidar-scaled fractional AOD with 07/2002–12/2003 data excluded as predictors; center: column MISR fractional AODs from all years as predictors; and right: GC-scaled MISR fractional AODs at ARM from all years as predictors.

Acknowledgments

References

Bey, I., Jacob, D. J., Yantosca, R. M., Logan, J. A., Field, B. D., Fiore, A. M., et al. (2001). Global modeling of tropospheric chemistry with assimilated meteorology: model description and evaluation. *Journal of Geophysical Research, [Atmospheres], 106* (D19), 23073−23095.

Campbell, J. R., Hlavka, D. L., Welton, E. J., Flynn, C. J., Turner, D. D., Spinhirne, J. D., et al. (2002). Full-time, eye-safe cloud and aerosol lidar observation at atmospheric radiation measurement program sites: instruments and data processing. *Journal of Atmospheric and Oceanic Technology, 19*(4), 431−442.

Diner, D., Beckert, J., Bothwell, G., & Rodriguez, J. (2002). Performance of the MISR instrument during its first 20 months in earth orbit. *IEEE Transactions on Geoscience and Remote Sensing, 40*(7), 1449−1466.

Engel-Cox, J. A., Hoff, R. M., Rogers, R., Dimmick, F., Rush, A. C., Szykman, J. J., et al. (2006). Integrating lidar and satellite optical depth with ambient monitoring for 3-dimensional particulate characterization. *Atmospheric Environment, 40*(40), 8056−8067.

Fairlie, T. D., Szykman, J., Gilliland, A., Bradley Pierce, R., Kittaka, C., Weber, S., et al. (2009). Lagrangian sampling of 3-D air quality model results for regional transport contributions to sulfate aerosol concentrations at Baltimore, MD, in summer 2004. *Atmospheric Environment, 43*(20), 3275−3288.

Ferrare, R., Turner, D., Clayton, M., Schmid, B., Redemann, J., Covert, D., et al. (2006). Evaluation of daytime measurements of aerosols and water vapor made by an operational Raman lidar over the Southern Great Plains. *Journal of Geophysical Research, [Atmospheres], 111*(D5).

Kahn, R., Banerjee, P., & McDonald, D. (2001). Sensitivity of multiangle imaging to natural mixtures of aerosols over ocean. *Journal of Geophysical Research, [Atmospheres], 106*(D16), 18219−18238.

Kahn, R., Banerjee, P., McDonald, D., & Diner, D. (1998). Sensitivity of multiangle imaging to aerosol optical depth and to pure-particle size distribution and composition over ocean. *Journal of Geophysical Research, [Atmospheres], 103*(D24), 32195−32213.

Kaufman, Y., Tanre, D., & Boucher, O. (2002). A satellite view of aerosols in the climate system. *Nature, 409*(6903), 215−223.

Lin, J. T., & McElroy, M. B. (2010). Impacts of boundary layer mixing on pollutant vertical profiles in the lower troposphere: implications to satellite remote sensing. *Atmospheric Environment, 44*(14), 1726−1739.

Liu, Y., Kahn, R., & Koutrakis, P. (2007a). Estimating PM2.5 component concentrations and size distributions using satellite retrieved fractional aerosol optical depth: part I — method development. *Journal of the Air & Waste Management Association, 57* (11), 1351−1359.

Liu, Y., Kahn, R., Turquety, S., Yantosca, R. M., & Koutrakis, P. (2007b). Estimating PM2.5 component concentrations and size distributions using satellite retrieved fractional aerosol optical depth: part II — a case study. *Journal of the Air & Waste Management Association, 57*(11), 1360−1369.

Liu, Y., Park, R. J., Jacob, D. J., Li, Q. B., Kilaru, V., & Sarnat, J. A. (2004). Mapping annual mean ground-level PM2.5 concentrations using Multiangle Imaging Spectroradiometer aerosol optical thickness over the contiguous United States. *Journal of Geophysical Research, [Atmospheres], 109*(D22) (Art. No. D22206).

Liu, Y., Sarnat, J., Kilaru, V., Jacob, D., & Koutrakis, P. (2005). Estimating ground-level PM2.5 in the Eastern United States using satellite remote sensing. *Environmental Science & Technology, 39*(9), 3269−3278.

Liu, Y., Schichtel, B. A., & Koutrakis, P. (2009). Estimating particle sulfate concentrations using MISR retrieved aerosol properties. *IEEE Journal of Selected Topics in Applied Earth Observations and Remote Sensing, 2*(3), 176−184.

Newsom, R. K., Turner, D. D., Mielke, B., Clayton, M., Ferrare, R., & Sivaraman, C. (2009). Simultaneous analog and photon counting detection for Raman lidar. *Applied Optics, 48*(20), 3903−3914.

Park, R. J., Jacob, D. J., Field, B. D., Yantosca, R. M., & Chin, M. (2004). Natural and transboundary pollution influences on sulfate-nitrate-ammonium aerosols in the United States: implications for policy. *Journal of Geophysical Research, [Atmospheres], 109*(D15) (Art. No. D15204).

Pope, C. A., & Dockery, D. W. (2006). Health effects of fine particulate air pollution: lines that connect. *Journal of the Air & Waste Management Association, 56*(6), 709−742.

Schmid, B., Ferrare, R., Flynn, C., Elleman, R., Covert, D., Strawa, A., et al. (2006). How well do state-of-the-art techniques measuring the vertical profile of tropospheric aerosol extinction compare? *Journal of Geophysical Research, [Atmospheres], 111* (D5) (Art. No. D05S07).

Schmid, B., Flynn, C. J., Newsom, R. K., Turner, D. D., Ferrare, R. A., Clayton, M. F., et al. (2009). Validation of aerosol extinction and water vapor profiles from routine Atmospheric Radiation Measurement Program Climate Research Facility measurements. *Journal of Geophysical Research, [Atmospheres], 114*, D22207.

van Donkelaar, A., Martin, R. V., & Park, R. J. (2006). Estimating ground-level PM2.5 using aerosol optical depth determined from satellite remote sensing. *Journal of Geophysical Research, [Atmospheres], 111*(D21) (Art. No. D21201).

Wang, J., Christopher, S. A., Nair, U. S., Reid, J. S., Prins, E. M., Szykman, J., et al. (2006). Mesoscale modeling of Central American smoke transport to the United States: 1. "Top-down" assessment of emission strength and diurnal variation impacts. *Journal of Geophysical Research, [Atmospheres], 111*(D5).

Welton, E. J., Voss, K. J., Quinn, P. K., Flatau, P. J., Markowicz, K., Campbell, J. R., et al. (2002). Measurements of aerosol vertical profiles and optical properties during INDOEX 1999 using micropulse lidars. *Journal of Geophysical Research-Atmospheres, 107*(D19).

Willis, A., Jerrett, M., Burnett, R. T., & Krewski, D. (2003). The association between sulfate air pollution and mortality at the county scale: an exploration of the impact of scale on a long-term exposure study. *Journal of Toxicology and Environmental Health. Part A, 66*(16-19), 1605−1804.

Wood, S. N. (2004). Stable and efficient multiple smoothing parameter estimation for generalized additive models. *Journal of the American Statistical Association, 99*(467), 673−686.